Effect of Trimetaphosphate and Fluoride Association on Hydroxyapatite Dissolution and Precipitation *In Vitro*

Alberto Carlos Botazzo Delbem[1], José Antonio Santos Souza[1], Ana Carolina Soares Fraga Zaze[2], Eliana Mitsue Takeshita[3], Kikue Takebayashi Sassaki[1], João Carlos Silos Moraes[4]

[1]Araçatuba Dental School, UNESP - Univ Estadual Paulista, Araçatuba, SP, Brazil
[2]Dental School, Paranaense University, Umuarama, PR, Brazil
[3]Dental School, UFS - Federal University of Sergipe, São Cristovão, SE, Brazil
[4]Engeneering School, UNESP - Univ Estadual Paulista, Ilha Solteira, SP, Brazil

Correspondence: Prof. Dr. Alberto Carlos Botazzo Delbem, Rua José Bonifácio 1193, 16015-050 Araçatuba, SP, Brazil. Tel.: +55-18-3636-3235. e-mail: adelbem@foa.unesp.br

The present study analyzed the action of sodium trimetaphosphate (TMP) and/or fluoride on hydroxyapatite. Hydroxyapatite powder was suspended in different solutions: deionized water, 500 µg F/mL, 1,100 µg F/mL, 1%TMP, 3%TMP, 500 µg F/mL plus 1%TMP and 500 µg F/mL plus 3%TMP. The pH value of the solutions was reduced to 4.0 and after 30 min, raised to 7.0 (three times). After pH-cycling, the samples were analyzed by X-ray diffraction and infrared spectroscopy. The concentrations of calcium fluoride, fluoride, calcium and phosphorus were also determined. Adding 1% or 3% TMP to the solution containing 500 µg F/mL produced a higher quantity of calcium fluoride compared to samples prepared in a 1,100 µg F/mL solution. Regarding the calcium concentration, samples prepared in solutions of 1,100 µg F/mL and 500 µg F/mL plus TMP were statistically similar and showed higher values. Using solutions of 1,100 µg F/mL and 500 µg F/mL plus TMP resulted in a calcium/phosphorus ratio close to that of hydroxyapatite. It is concluded that the association of TMP and fluoride favored the precipitation of a more stable hydroxyapatite.

Introduction

In human tooth enamel, hydroxyapatite (HA – $Ca_{10}(PO_4)_6(OH)_2$) crystals are arranged into highly organized prisms to for the main unit. In the oral cavity, tooth enamel can be damaged by the local cariogenic bacteria in biofilm (caries) or non-bacterially derived erosive challenges (such as acidic beverages) (1). The process of dental caries is characterized by the dissolution of hydroxyapatite (HA) from tooth enamel. The maintenance of that component in dental structures by decreasing its dissolution can be achieved by using fluoride (F)-containing products (2). In order to become less dependent of F-based items, combinations of different non–fluoride agents and F have been studied (3). Some studies have shown that inorganic phosphates have anticariogenic action (4). Among them, sodium trimetaphosphate (TMP) seems to be the most active. The mechanism by which TMP reduces the dissolution of HA has not been completely clarified. The literature suggests that it is related to TMP adsorption by the enamel surface (4), thus causing a reduction in ion exchange between the enamel and the oral environment, thereby reducing demineralization during acidic challenge.

The addition of TMP to dentifrices with low F concentrations has shown the potential of TMP as a caries-preventing (5,6) and anti-erosion agent (7,8). The results of an *in vitro* study (9) showed that this combination avoids laminated caries lesion formation, as has already been observed in another study (10). However, to obtain new information on the TMP mechanism of caries prevention, an analysis of the effects of TMP on the dissolution behavior of HA is important in order to verify the changes that can occur during the demineralization and remineralization process in the simultaneous presence of the two components, TMP and F. Moreover, the studies assessing the effects of F and TMP in the dynamics of dental caries and erosion cited above does not considered the direct interactions between F and TMP with dental enamel. Thus, in the present study, we used HA powder and an *in vitro* model to simulate the dissolution and precipitation of HA. This allows us to investigate the mechanisms by which TMP and/or F affect the HA structure.

Method and Materials

Synthesis of HA

HA powders were prepared based on the synthesis route published by Qu and Wei (11) and Rintoul et al. (12). Calcium nitrate [$Ca(NO_3)_2 \cdot 4H_2O$, 1 mol/L, 300 mL, Sigma-Aldrich Co., St. Louis, MO, USA] and dibasic ammonium phosphate [$(NH_4)H_2PO_4$, 0.3 mol/L 600 mL, Sigma-Aldrich] solutions were prepared. The pH values of both solutions were adjusted to 10–12 by adding concentrated ammonium hydroxide (29.5%). The dibasic ammonium phosphate solution was slowly added to the calcium nitrate solution (2–5 mL/min) under constant agitation at 37 °C. The precipitate was subsequently aged for 7 days at 37 °C and ground into a fine powder (synthetic HA) (13).

A.C.B. Delbem et al.

Demineralization and Treatment

Pure TMP solutions (100 mL $Na_3P_3O_9$; Sigma-Aldrich) at concentrations of 1.0% and 3.0% and the corresponding TMP solutions with added sodium fluoride (500 μg F/mL), were prepared(5). As a positive control, a solution of 1,100 μg F/mL (NaF, Merck, Darmstadt, Germany) was also prepared. The HA powder (0.5 g) (n=5) was suspended in each experimental solution of TMP and/or F for 30 min at a pH value of 7.0. Aliquots of HA powder were also suspended in deionized water and were used as negative controls (HA_{NC}).

After preparation of the solutions, the pH value of each solution was slowly reduced to 4.0 using 1 mol/L nitric acid (HNO_3, Merck) under agitation. After 30 min of equilibration, the pH value of each solution was raised to 7.0 by the addition of 1 mol/L sodium hydroxide (NaOH; Merck). The pH cycling process was repeated three times, ending at pH=7.0 at 37 °C (11,12). The resulting precipitates were filtered and washed five times with deionized water. The solid phase was oven dried for 24 h at 70 °C and ground into a fine powder using an agate mortar and a pestle. Particles of diameter 53 μm were isolated and analyzed using X-ray diffraction (XRD), Fourier-transform infrared (FTIR) spectroscopy, and fluoride (F), calcium (Ca) and phosphorus (P) analysis.

FTIR Spectroscopy and XRD

For each solution subjected to pH cycling, two HA samples were analyzed by FTIR spectroscopy. The IR absorption spectra of the samples were recorded using a diffuse reflectance method on an FTIR spectrophotometer (Nexus 670; Nicolet, Ramsey, MN, USA), performing 128 scans at a resolution of 2 cm^{-1} in a spectral range of 4000–400 cm^{-1}. The intensities of the absorption bands were measured relative to a baseline by joining the points of lowest absorbance of a given peak. The intensity values obtained in this way were all expressed as percentages (%) and compared to those of HA_{NC}(13). XRD data were obtained using Cu-Kα radiation (Ultima IV X-ray diffractometer; Rigaku Corp., Osaka, Japan) generated at a voltage of 40 kV and a current of 40 mA. The XRD patterns were obtained in a scanning range (2θ) from 10° to 60°, with a step size of 0.02°. The CRYSTMET database (Toth Information Systems Inc., Ottawa, Canada) was used for phase identification.

Analysis of Loosely bound (CaF₂) and Firmly Bound Fluoride (FA-like) in HA

Assessment of the uptake of loosely bound fluoride (alkali-soluble fluoride, CaF_2) by HA was performed following the method of Caslavska et al.(14). For this purpose, 5 mg of cycled HA powder were weighed in microtubes and 0.5 mL of 1.0 mol/L potassium hydroxide were added. After 24 h of stirring (Orbital Shaker TE-141; Tecnal, Piracicaba, SP, Brazil), the suspension was centrifuged at 2900 g for 20 min; 0.3 mL of the supernatant were neutralized by 0.3 mL of TISAB II (ionic strength adjuster buffer, pH 5.0) modified with 1.0 mol/L HCl. The fluoride concentration was determined using an F-selective electrode (Orion 9409, Orion Research Inc., Beverly, MA, USA), which had previously been calibrated. The firmly bound fluoride (fluorapatite-like, FA-like) was measured in the precipitates, which were washed three times in distilled/deionized water and once in methanol. After methanol evaporation, 0.25 mL of 1.0 mol/L HCl were added to the microtube. After stirring for 1 h, 0.25 mL of TISAB II modified by 20 g of NaOH/L were added. Duplicate samples were analyzed as described previously.

HA Calcium and Phosphorus Analysis

For the determination of the Ca and P content, 0.5 mL of 1.0 mol/L hydrochloric acid were added to 5 mg of each of the pH-cycled HA samples in microtubes. After stirring for 1 h, the samples were neutralized with 0.5 mL of 1.0 mol/L NaOH. The Ca concentration was analyzed by the Arsenazo III colorimetric method (15) using a $CaCl_2$ standard (40–200 μg Ca/mL). The P content was determined by the molybdate method using a KH_2PO_4 (1.5–24 μg P/mL) standard (16). All reactions were performed in 96-well plates and the absorbance data were measured in a microplate spectrophotometer (PowerWave 340; BioteK, Winooski, VT, USA) at 650 nm (Ca) and 660 nm (P).

Data Analysis

The FTIR spectroscopic data were analyzed as a function of the presence and intensities (%) of the spectral bands of the HA samples subjected to pH-cycling in comparison to the negative control (HA_{NC}). The results of the concentrations, expressed as mg/g, of F (CaF_2 and FA-like), Ca, and P in HA were subsequently tested for normality (Shapiro–Wilk test) and homogeneity (Cochran test). P and F (log_{10} transformation) data were subjected to variance analysis (one-way), followed by the Student–Newman–Keuls test. The Ca data showed a heterogeneous distribution and were submitted to the Kruskal–Wallis test, followed by the Student–Newman–Keuls test. Statistical analysis was performed using the program SigmaPlot version 12.0 (Systat Software Inc., USA), and the significance level was set at 5%.

Results

The measured XRD pattern of synthetic HA was in agreement with the reference diffractogram of HA, according to the CRYSTMET database. No qualitative difference was observed between XRD pattern of the

HA_{NC} and pure HA specimens (Fig. 1A) as well as between the pure HA and 1%TMP and 3%TMP (Fig. 1B). Traces of CaF2 were found in the HA and HA_{NC} patterns. This phase (◊) was easily identified in the XRD pattern of the HA dispersed in the solution at a concentration of 1,100 µg F/mL (F1100 pattern). The F1100 showed sharper peaks than those of the samples of pure HA and HA_{NC} (to see inset of the Fig. 1A). This narrowing of the peaks is an indicative of the increased crystallinity of HA. Based on the Scherrer equation, $D=0.9\lambda/\beta cos\theta$ (λ is the X-ray wavelength, β is the line broadening at half the maximum intensity (FWHM) in radians and θ is the Bragg angle), the size (D) of crystallites estimated by us was 20 nm for HA and 34 nm for F1100 samples. Treatment with 500 µg F/mL and 1% or 3% TMP also produced sharper peaks than those of pure HA (Fig. 1b).

The IR spectra of the seven analyzed spectra show typical peaks of carbonated HA in the regions 550–700 cm^{-1} (v_4) and 900–1350 cm-1 (v_1 and v_3), which correspond to phosphate bands; the carbonate v_2 vibrational mode is located at 868–897 cm^{-1}, and the v_3 vibrational mode of the carbonate ion is found in the region 1360–1550 cm^{-1} (Fig. 2). In calcium-deficient HA, the v_2 vibrational excitation band of CO_3^{2-} may be superimposed on a symmetrical stretching vibration (v_5) of the HPO_4^{2-} group. Furthermore, the spectra contain OH bands, typically observed at 642–663 cm^{-1} (OH liberation band), a deformation band at 1639–1651 cm^{-1}, and two OH stretching bands at 3570 cm^{-1} (narrow band) and in the region 3350–3454 cm^{-1} (broad band). The intensities of the two phosphate bands at lower frequencies increased for the HA samples treated with combined solutions of fluoride (1,100 and 500 µg F/mL) and 1%TMP, and decreased in the presence of 1% and 3% pure TMP solutions (Fig. 3A). The three carbonate bands showed a stronger decrease upon treatment with

1,100 and 500 µg F/mL and 1%TMP, compared to HA_{NC} (Fig. 3B). The OH vibrational and stretching (3570 cm^{-1}) bands decreased in intensity, irrespective of the treatment (Figs. 2 and 3A). The 1,100 and 500 µg F/mL plus 1%TMP
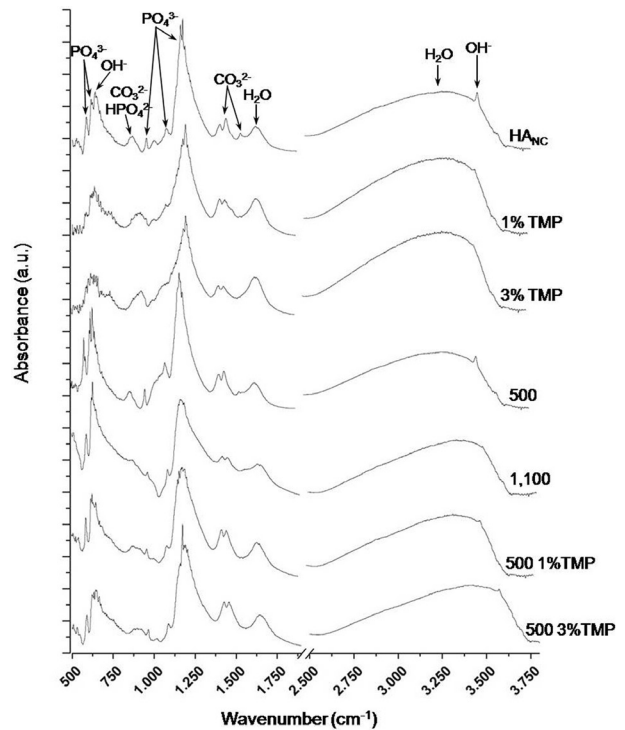

Figure 2. FTIR spectra according to groups after pH cycling: HA_{NC}=HA powder suspended in deionized water; 1% TMP=HA powder suspended in solution of 1% TMP; 3% TMP=HA powder suspended in solution of 3% TMP; 500=HA powder suspended in solution of 500 µg F/mL; 1,100=HA powder suspended in solution of 1,100 µg F/mL; 500 1%TMP=HA powder suspended in solution of 500 µg F/mL associated to 1% TMP; 500 3%TMP=HA powder suspended in solution of 500 µg F/mL associated to 3% TMP.
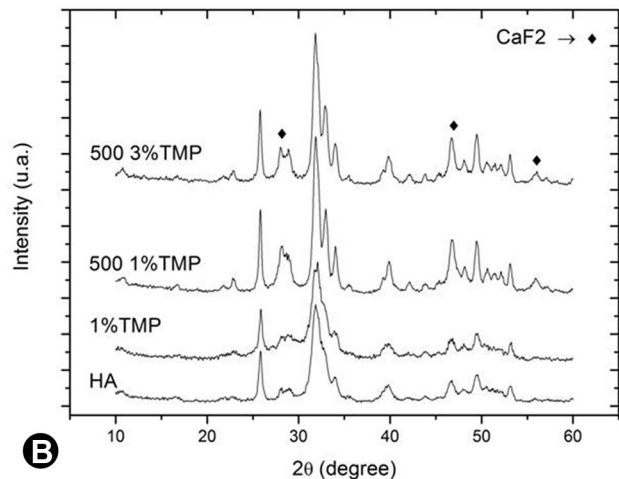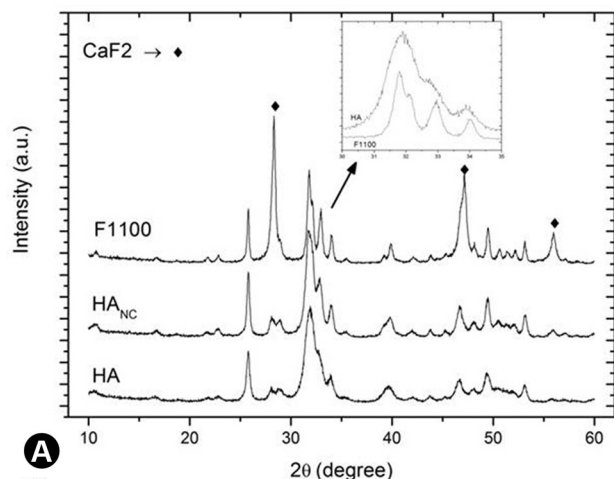
Effect of trimetaphosphate on hydroxyapatite

Figure 1. A: XRD patterns of the prepared hydroxyapatite (HA), demineralized HA (HA_{NC}) and HA treated with 1,100 µg F/mL (1,100). B: HA, HA treated with 1% TMP (1% TMP), HA with 500 µg F/mL and 1%TMP (500 1%TMP) and HA with 500 µg F/mL and 1%TMP (500 3%TMP).

treatments always led to lower intensities.

Chemical analysis showed higher Ca concentrations in HA when treated in solutions of 1,100μg F/mL, 500 μg F/mL and 1%TMP, and 500 μg F/mL and 3%TMP (Table 1) compared with the other samples (p<0.001). The combination of 500 μg F/mL and TMP resulted in Ca/P ratios similar to that of pure HA. Fluoride-treated samples had higher values of CaF$_2$ and FA-like than the samples without F (p<0.05). The combination of F and TMP enabled CaF$_2$ formation at rates two and four times higher than for HA treated in pure fluoride solutions of 1,100 and 500

μg F/mL (p<0.001), respectively (Table 1). Increasing the F concentration in solution (from 500 μg F/mL to 1,100 μg F/mL) also increased the FA-like content in HA by a factor of two. The combination of F and TMP did not increase the values of FA-like, but reduced it for a solution of 3% TMP.

Discussion

According to Rintoul et al. (12) and Sundaram et al. (17), the presence of OH bands in the frequency range 642–663 cm^{-1} indicates HA precipitation, as observed in the present study. Despite lower Ca concentrations and Ca/P ratios, mainly in the HA$_{NC}$ samples, calcium-deficient HA can show the same crystalline arrangement as stoichiometric HA (13,18). Fluoride incorporation in apatite structures increases the crystallinity and the calcium phosphate amount (19). This was observed when hydroxyapatite was pH-cycled in the presence of 1,100 μg F/mL. The increase in the F concentration and the intensity decrease of the OH bands (at 642–663 cm^{-1} and 3570 cm^{-1}, respectively) in the IR spectra indicate the presence of F ions in HA(17,20). The reduction in the number of OH groups may suggest that F- is linked to OH, without replacing it, indicating the precipitation of fluoridated HA with a high Ca/P ratio and good crystallinity. Two data support this assertion: (a) the correlation between the IR intensity of the OH group in the 642–663 cm^{-1} region and the FA-like concentration (r=-0.836, p=0.038) and (b) the absence of a peak (745–747 cm^{-1}) indicating F replacement in any spectrum (Fig. 3) (12,17). On the other hand, calcium fluoride formation did not show a correlation with the OH bands. The large calcium fluoride amount found in HA when treated with a combined solution of F and TMP could be one of the factors that may explain the better results obtained by Takeshita et al. (5,9).

Table 1. Concentration (mg/g) of Loosely-bound (CaF$_2$) and firmly-bound fluoride (FA-like), calcium (Ca) and phosphorus (P), and Ca/P molar ratio according to the experimental groups (n = 5)

Groups	CaF$_2$	FA-like	Ca	P	Ca/P
HA	0.008[a] (0.002)	0.001[a] (0.000)	373.9[a] (27.1)	202.4[a] (12.3)	1.56[a,c] (0.09)
HA$_{NC}$	0.005[b] (0.001)	0.001[a] (0.000)	237.5[b] (21.6)	194.2[a,d] (7.3)	1.15[b] (0.08)
1%TMP	0.003[c] (0.001)	0.002[a] (0.000)	334.6[c] (20.5)	153.6[b] (14.1)	1.61[a] (0.07)
3%TMP	0.005[b] (0.001)	0.002[b] (0.001)	268.5[d] (9.9)	137.3[c] (8.1)	1.49[a,c] (0.08)
500	7.719[d] (0.374)	5.580[c] (0.688)	317.0[c] (4.4)	184.9[d] (12.8)	1.43[c] (0.08)
1100	12.519[e] (0.718)	9.871[d] (1.717)	362.9[a] (8.8)	147.0[b,c] (11.5)	1.68[a] (0.08)
500 1%TMP	29.387[f] (0.999)	5.521[c] (1.921)	395.2[a] (59.3)	172.2[e] (7.6)	1.60[a] (0.01)
500 3%TMP	29.064[f] (4.256)	2.927[e] (0.716)	362.9[a] (19.6)	171.8[e] (16.9)	1.57[a,c] (0.02)

Data are expressed as means (S.D.). Means followed by different small letters indicate statistical difference between groups in each analysis (Student-Newman-Keuls test, p < 0.001).
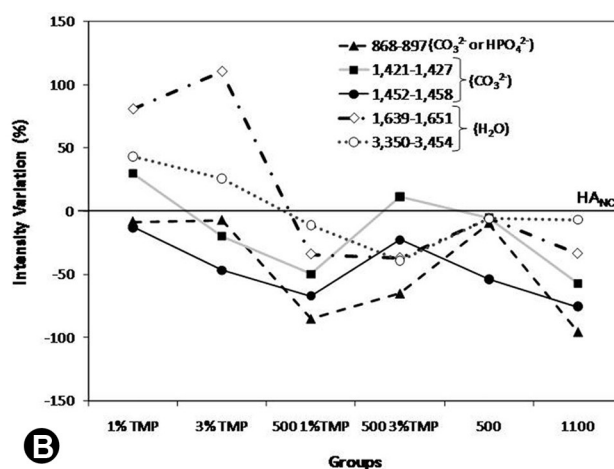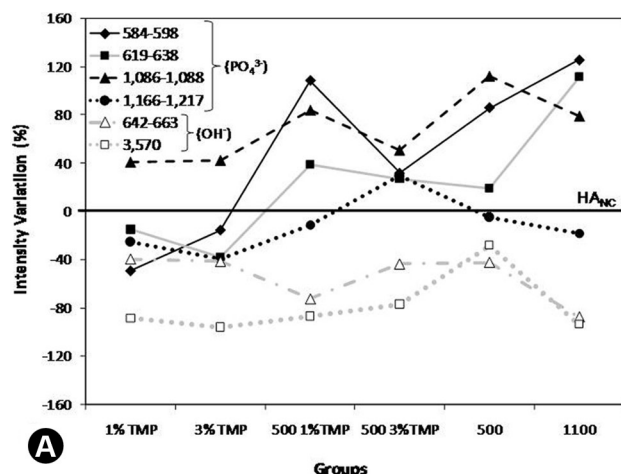

Figure 3. Intensity variation (%) of the hydroxyapatite bands submitted to treatments (1%TMP, 3%TMP, 500 1%TMP, 500 3%TMP, 500 and 1,100) in relation to HA$_{NC}$. A: The intensities of the phosphate and hydroxyl bands. B: Intensity variation of carbonate and water groups.

The narrow OH stretching band is associated with free OH- ions (21,22) and the broad band with the existence of lattice or adsorbed water in the samples(24). As in the case of the F group, the intensity of the narrow OH band also decreased in the presence of TMP. However, a correlation was only observed for the intensity of the OH bands in the regions 642–663 cm^{-1} and 3570 cm^{-1} (r=0.746; p=0.033) and fluoride. The intensity reduction of the narrow OH band upon TMP treatments indicates the hydroxyl binding site of TMP on HA. Two data support this hypothesis: (a) there is a reduction in the concentration of FA-like with increasing TMP and its associated F concentration and (b) the intensity of the narrow OH band is smaller in the presence of TMP. This indicates competition for the same binding site between TMP and F in HA.

Although the IR spectra indicate an intensity increase of most phosphate bands, the chemical analysis showed a reduction in the P concentration in F groups, mainly for the samples treated in a solution of 1,100 µg F/mL. This decrease could be related to P in the form of HPO_4^{2-} replacing PO_4^{3-} sites (23), whose band shows a greater intensity reduction in fluoride-treated HA compared with samples prepared in solutions of 1% and 3% TMP. The HPO_4^{2-} band is related to the formation of calcium-deficient HA (Ca/P 1.5–1.6) synthesized in this experiment(21). The corresponding peak intensity is higher for a lower Ca/P ratio or Ca concentration (21,22). These data are in agreement with the results obtained by FTIR spectroscopy and chemical analysis.

A reduction of calcium loss by adsorption of TMP and/or fluoride on HA results in a concomitant intensity decrease of the carbonate v_3 band. A higher concentration of Ca in HA can produce a positive charge deficit, which is counterbalanced by the release of carbonate from the HA crystal (24). This effect varies with the concentration of TMP and associated F in the solutions, resulting in different carbonate structures. The reduction of P and the increase of Ca in HA can explain the best Ca/P ratio being observed in the presence of TMP and/or F, and the increase in crystallinity, as observed by XRD.

It is important to mention that in this study an *in vitro* model and a HA powder was used to simulate cariogenic challenge (process of de-remineralization) for the evaluation of the effect of TMP and/or F on HA. However, this is a chemical model and therefore it presents limitations, especially related to the inability to reproduce the complex intraoral conditions. Such as, the saliva and the acquired pellicle are extremely important in the de- and remineralization process as well for adsorption of ions and molecules to the HA structure (25).

Our study shows that TMP associated with 500 µg F/g reduces the demineralization of HA and decreases Ca loss, improving the HA crystallinity. Furthermore, the adsorption

of calcium fluoride on the crystal structure is increased. TMP and fluoride compete for the same binding sites in the hydroxyapatite.

Resumo

O presente estudo avaliou a ação do trimetafosfato de sódio (TMP) e/ou fluoreto sobre a hidroxiapatita. Pó de hidroxiapatita foi suspenso em diferentes soluções: água deionizada, 500 µg F/mL, 1100 µg F/mL, 1%TMP, 3%TMP, 500 µg F/mL adicionado a 1%TMP e 500 µg F/mL associado a 3%TMP. O pH das soluções foi reduzido para 4,0 e depois de 30 min, elevado para 7,0 (três vezes). Depois do processo de ciclagem de pH, as amostras foram analisadas por difração de raios-X e espectroscopia por infravermelho. As concentrações de fluoreto de cálcio, fluoreto, cálcio e fósforo também foram determinadas. A adição de 1% ou 3% TMP na solução contendo 500 µg F/mL produziu uma maior quantidade de fluoreto de cálcio comparado às amostras tratadas com uma solução de 1100 µg F/mL. A respeito da concentração de cálcio, amostras tratadas com soluções de 1100 µg F/mL e 500 µg F/mL adicionado ao TMP foram estatisticamente similares e mostraram maiores valores. Soluções de 1100 µg F/mL e 500 µg F/mL adicionado ao TMP resultaram em uma proporção molar Ca/P mais próxima à da hidroxiapatita. Conclui-se que a associação de TMP e F favoreceu a precipitação de uma hidroxiapatita mais estável.

Acknowledgements

References

1. Duo W, Jiaojiao Y, Jiyao L, Liang C, Bei T, Xyngyu C, et al.. Hydroxyapatite-anchored dendrimer for *in situ* remineralization of human tooth enamel. Biomaterials 2013;31:5036–5047.

2. Stookey GK, Mau MS, Isaacs RL, Gonzales-Gierbolini C, Bartizek RD, Biesbrock AR. The relative anticaries effectiveness of three fluoride-containing dentifrices in Puerto Rico. Caries Res 2004;38:542–550.

3. Rethman MP, Beltrán-Aguilar ED, Billings RJ, Hujoel PP, Katz BP, et al.. Non-fluoride caries-preventive agents: executive summary of evidence-based clinical recommendations. J Am Dent Assoc 2011;142:1065–1071.

4. Gonzalez M, Jeansonne BG, Feagin FF. Trimetaphosphate and fluoride actions on mineralization at the enamel-solution interface. J Dent Res 1973;52:261–266.

5. Takeshita EM, Castro LP, Sassaki KT, Delbem ACB. *In vitro* evaluation of dentifrice with low fluoride content supplemented with trimetaphosphate. Caries Res 2009;43:50–56.

6. Amaral JG, Freire IR, Valle-Neto EFR, Cunha RF, Martinhon CCR, Delbem ACB. Longitudinal evaluation of fluoride levels in nails of 18-30-month-old children that were using toothpastes with 500 and 1100 µgF/g. Community Dent Oral Epidemiol 2014;42:412-419.

7. Moretto MJ, Magalhães AC, Sassaki KT, Delbem AC, Martinhon CC. Effect of different fluoride concentrations of experimental dentifrices on enamel erosion and abrasion. Caries Res 2010;44:135–140.

8. Manarelli MM, Vieira AE, Matheus AA, Sassaki KT, Delbem AC. Effect of mouth rinses with fluoride and trimetaphosphate on enamel erosion: an *in vitro* study. Caries Res 2011;45:506–509.

9. Takeshita EM, Exterkate RA, Delbem AC, ten Cate JM. Evaluation of different fluoride concentrations supplemented with trimetaphosphate on enamel de- and remineralization *in vitro*. Caries Res 2011;45:494–497.

10. ten Cate JM, Buijs MJ, Chaussain Miller C, Exterkate RAM. Elevated

Effect of trimetaphosphate on hydroxyapatite

fluoride products enhance remineralization of advanced enamel lesion. J Dent Res. 2008;87:943–947.

11. Qu H, Wei M. Synthesis and characterizations of fluorine-containing hydroxyapatite by a pH-cycling method. J Mater Sci Mater Med 2005;16:129–133.

12. Rintoul L, Wentrup-Byrne E, Suzuki S, Grondahl L. FT-IR spectroscopy of fluorosubstituted hydroxyapatite: strengths and limitations. J Mater Sci Mater Med 2007;18:1701–1709.

13. Delbem AC, Alves KM, Sassaki KT, Moraes JC. Effect of iron II on hydroxyapatite dissolution and precipitation *in vitro*. Caries Res 2012;46:481–487.

14. Caslavska V, Moreno EC, Brudevold F. Determination of the calcium fluoride formed from *in vitro* exposure of human enamel to fluoride solutions. Arch Oral Biol 1975;20:333–339.

15. Vogel GL, Zhang Z, Carey CM, Ly A, Chow LC, Proskin HM. Composition of plaque and saliva following use of a tricalcium-phosphate-containing chewing gum and a subsequent challenge. J Dent Res 2000;79:58–62.

16. Fiske CH, Subarrow Y. The colorimetric determination of phosphorus. J Biol Chem 1925;66:375–400.

17. Sundaram CS, Viswanathan N, Meenakshi S. Defluoridation chemistry of synthetic hydroxyapatite at nano scale: equilibrium and kinetic studies. J Hazardous Mater 2008;155:206–215.

18. Ishikawa K, Ducheyne P, Radin S. Determination of the Ca/P ratio in calcium-deficient hydroxyapatite using X-ray diffraction analysis. J Mater Sci Mater Med 1993;4:165–168.

19. van den Hoek WGM, Feenstra TP, De Bruyn PL. Influence of fluoride on the formation of calcium phosphate in moderately supersaturated solutions. J Phys Chem 1980;84:3312–3317.

20. Jha LJ, Best SM, Knowles JC, Rehman I, Santos JD, Bonfield W. Preparation and characterization of fluoride-substituted apatites. J Mater Sci Mater Med 1997;8:185–191.

21. Elliott JC. Hydroxyapatite and non-stoichiometric apatites. In: Elliott JC, editor. Structure and Chemistry of the Apatites and Other Calcium Orthophosphates. Amsterdam: Elsevier; 1994.

22. Coates J. Interpretation of infrared spectra, a practical approach. In: Meyers RA, editor. Encyclopedia of analytical chemistry. New York: John Wiley & Sons; 2000.

23. Kumar GS, Girija EK, Thamizhavel A, Yokogawa Y, Kalkura SN. Synthesis and characterization of bioactive hydroxyapatite-calcite nanocomposite for biomedical applications. J Colloid Interface Sci 2010;349:56–62.

24. Wopenka B, Pasteris JD. A mineralogical perspective on the apatite in bone. Mater Sci Eng C 2005;25:131–143.

25. Souza JAS, Amaral JG, Moraes JCS, Sassaki KT, Delbem ACB. Effect of sodium trimetaphosphate on hydroxyapatite solubility: An *in vitr*o study. Braz Dent J 2013;24:235-240.